Available online at www.sciencedirect.com
ScienceDirect
International Journal of Mass Spectrometry 261 (2007) 140–145
International Journal of Mass Spectrometry
www.elsevier.com/locate/ijms

Two-laser mid-infrared and ultraviolet matrix-assisted laser desorption/ionization

Mark W. Little, Kermit K. Murray *

Louisiana State University, Baton Rouge, LA 70803, USA

Received 18 May 2006; received in revised form 19 August 2006; accepted 21 August 2006
Available online 26 September 2006

Abstract

Matrix-assisted laser desorption/ionization (MALDI) was performed using two-pulsed lasers with wavelengths in the infrared and ultraviolet regions. A 2.94 μm pulsed optical parametric oscillator laser system and a 337 nm pulsed nitrogen laser irradiated the same spot on the sample target. Sinapinic acid (SA), 2,5-dihydroxybenzoic acid (DHB), α-cyano-4-hydroxycinnamic acid (CCA), and 4-nitroaniline (NA) were used as matrices, and bovine insulin and cytochrome C were used as analytes. The laser energy was adjusted so that one-laser MALDI and LDI was at a minimum and the matrix and analyte ion signal was enhanced when the two lasers were fired together. Two-laser LDI was observed with SA, DHB, and NA matrices and two-laser MALDI was observed with SA and DHB. Plots of ion signal as a function of delay between the IR and UV lasers show two-laser signal from 0 ns up to a delay of 500 ns when the IR laser is fired before the UV laser. The results are interpreted in terms of IR laser heating of the target that leads to an enhancement in UV LDI and MALDI.

Keywords: MALDI; Laser desorption ionization; Infrared; Mechanism

1. Introduction

Two-pulse matrix-assisted laser desorption/ionization (MALDI) involves ion formation using two-laser pulses, both of which are below the threshold fluence for analyte ion formation [1–4]. Two-pulse MALDI can be carried out using one laser and an optical delay line, two lasers of the same wavelength or two lasers of different wavelength. The first pulse irradiates a spot on the sample and ionization proceeds after irradiation of the same spot by a second pulse. Ion signal can be observed in some cases even if the lasers are delayed in time with respect to each other. By measuring the ion signal, as a function of the delay, information about the time behavior of MALDI ion formation can be obtained. Because matrix and analyte ion formation are closely related, two-pulse MALDI is often studied by monitoring both the matrix and analyte ion signal.

Initial two-pulse MALDI studies were performed with laser pulses of the same ultraviolet (UV) wavelength [1–3]. The first such study used two 337 nm nitrogen lasers with 5 ns pulse widths for two-laser MALDI [1]; the protein bovine insulin in sinapinic acid (SA), 6-aza-2-thiothymine and 2,5-dihydroxybenzoic acid (DHB) matrices and the oligonucleotide decathymidylic acid in 3-hydroxypicolinic acid matrix were tested. Depending on the matrix, maximum analyte ion signal was recorded at delays between 5 and 10 ns and decayed to zero within 30 ns. Maximum analyte ion signal at non-zero delay was explained by delayed production of the precursor ions that result in the production of analyte molecules. The role of electronically excited matrix was also considered. Two-pulse MALDI MS with a single laser was carried out using a single 337 nm nitrogen laser with a 4 ns pulse width and an optical delay line [3]. Exponential decay of analyte ion signal with a time constant of 4–5 ns was observed for DHB and SA matrix. However, with 9-anthracenecarboxylic (9-ACA) and α-cyano-4-hydroxycinnamic acid (CCA), a delay of 3.2 and 6.1 ns was required to achieve maximum signal. The difference among the various matrices was attributed to variations in the desorption plume density affecting the rate of proton transfer reactions.

Faster processes can be studied using short pulse lasers. In one study a 30 ps pulse width 355 nm Nd:YAG laser with an optical delay line was used to investigate LDI of the DHB matrix itself [2]. Matrix ion formation processes with a short and long time behavior were observed. With the fast process, matrix ion

* Corresponding author.
E-mail address: kkmurray@lsu.edu (K.K. Murray).

1387-3806/$ – see front matter © 2006 Elsevier B.V. All rights reserved.
doi:10.1016/j.ijms.2006.08.010

signal is observed at $t = 0$ and this signal decays rapidly to a local minimum near 150 ps. The slower process leads to an increase in matrix ion signal to a maximum at a delay of 2 ns, after which the matrix ion signal drops to zero after a delay of 8 ns. The slow process can be explained either by physical or chemical changes in the DHB matrix after irradiation. The possibility of a delayed gas phase ion formation was also noted. Since both lasers were directed at the same location on the sample target, irradiation of desorbed sample material by the second laser pulse might have occurred several micrometers above the sample surface given an initial DHB neutral velocity of approximately 1000 m/s. Ionization of the desorbed sample material is then determined by the transfer rate of the solid into the gas phase.

Two-pulse MALDI MS has been performed with two lasers with two different wavelengths, one in the IR and one in the UV: a CO_2 laser operating at 10.6 μm and a nitrogen laser operating at 337 were used [4]. The CO_2 laser pulse consisted of an initial 80 ns pulse with 40% of the laser energy followed by tail out to 900 ns. The protein bovine insulin in DHB matrix was analyzed. No ion signal was observed until a delay of ~700 ns and maximum matrix and analyte ion signal was found at a delay of ~1 μs. The ion signal decayed to zero after a delay of 200–400 μs. The microsecond delay in two-laser MALDI is consistent with heating, and possibly melting, of the matrix by infrared (IR) laser heating followed by more efficient ionization by the UV laser. Maximum matrix and analyte ion signals were observed after all the IR laser energy had been deposited in the target, coincident with the maximum target temperature according to a simple one-dimensional model for laser heating. The decay of the ion signal was interpreted as a decrease in two-pulse ionization efficiency due to cooling of the target and formation of solid matrix.

A proportional dependence of ionization efficiency on sample temperature has also been observed with static target studies of UV MALDI. In one study, the threshold fluence for 337 nm MALDI was recorded at temperatures between −100 and 20 °C; more efficient ionization (as indicated by low threshold fluence) was found for matrix ions as the temperature increased [5]. Another study measured the effect of increasing the sample temperature from room temperature to 160 °C on DHB matrix ion production at 337 nm [6]. A general trend of increasing matrix ion signal was found up to 120 °C followed by a slight decrease at higher temperatures.

In this study, two-pulse LDI was carried out using a 5 ns pulse width optical parametric oscillator (OPO) operating at 2.94 μm and a 4 ns pulse width nitrogen laser at 337 nm. Our goal was to test the hypothesis that the IR laser heats the sample, followed by more efficient UV MALDI of the transiently heated sample. The peptides gramicidin S and bradykinin and the proteins bovine insulin and cytrochrome C were tested in DHB, SA, CCA and 4-nitroaniline matrices. Plots of ion signal area versus delay were recorded for matrix and analyte ions.

2. Experimental

2.1. Mass spectrometry

The instrument used in this experiment was a linear time-of-flight mass spectrometer operated under positive and static ion extraction conditions [7]. Ions were accelerated with a total kinetic energy of 20 keV before entering a 1 m field free region and received 2 keV of post acceleration before impinging on a dual 25 mm microchannel plate detector. Mass spectra were acquired using a digital oscilloscope and represent an average of ten laser shots.

2.2. Two-laser arrangement

The two-laser arrangement has been described previously [4]. In this study, the pulsed IR source was a tunable OPO (Mirage 3000B, Continuum, Santa Clara, CA, USA) pumped by 1064 nm fundamental and 532 nm second harmonic of an Nd:YAG laser (Powerlite 8000, Continuum, Santa Clara, CA, USA). The OPO output is a 5 ns laser pulse tunable from 1.45 to 4.0 μm; a wavelength of 2.94 μm was used for all experiments. A 2.5 μm long pass filter with 80% transmission (FXLP-0250, Janos Technologies, Keene, NH) was used to block the pump laser and other wavelengths. The IR laser was focused using a 254 mm CaF_2 lens to a spot size of 200 μm × 300 μm determined using laser burn paper and a measuring microscope. The laser beam profile is Gaussian; no beam homogenization was performed. The IR laser entered the ion source at a 45° angle through a sapphire vacuum window. The laser pulse energy was attenuated using a variable iris, which produced a laser fluence of 1000 J/m^2 for all experiments except for DHB where a laser fluence of 2100 J/m^2 was used. The laser energy was measured using a pyroelectric joulemeter (ED-104AX, Gentec, Palo Alto, CA, USA).

A 4 ns pulse width, 337 nm nitrogen laser (VSL-337ND-S, LSI, Franklin, MA, USA) was used as the UV laser source. Attenuation was achieved using a variable iris and a variable circular neutral density filter (50Q04AV.1, Newport, Irvine, CA, USA) mounted on a rotating stage. The UV laser was focused using a 254 mm focal length fused-silica lens to a spot size of 100 μm × 200 μm determined with the laser burn paper and measuring microscope. A laser fluence of 300 J/m^2 was used for all experiments except for 4-nitroaniline samples where a 60 J/m^2 fluence was used. UV laser light entered the ion source through a 45° quartz vacuum window, and the angle between the UV and IR laser was 90°.

The two-laser beams were focused to the same location on the sample target and a CCD camera with a macro zoom lens were used to observe coarse beam overlap. The IR and UV laser beams were adjusted until both burned the same spot on the laser burn paper. Fine overlap was achieved by adjusting one beam to maximize two-laser ion signal with 4-nitroaniline. Alignment of the beams was carried out each day of experiments.

2.3. Data acquisition

The automated method for data acquisition has been described previously [4]. Data for integrated ion signal as a function of delay (Δt) were obtained between −300 and 900 ns in 100 ns increments for bovine insulin in SA matrix and −70 to 950 ns in 10 ns increments for 4-nitroaniline. Shorter time increments were possible for matrix time plots due to the greater signal intensity and stability. A positive Δt indicates that the IR

is fired before the UV and a negative Δt indicates UV firing before IR. The integration limits were 1 μs for bovine insulin and 60 ns for NA and were chosen to encompass the given peak from baseline to baseline. Three to five single shot spectra were averaged. The sequence of data acquisition over the full range of delay times was automatically repeated five times. Each data point resulted from an average of 15–25 laser shots. Roughly twenty percent of the data points were removed as outliers in accordance with a standard *t*-test. The delay was calibrated daily using photodiodes (ET-2000, Electro-Optics Technology, Inc., Traverse City, MI, USA) to measure the nitrogen laser light and the 532 nm OPO pump laser light. The time jitter between the two pulses was 40 ns, which was limited by the nitrogen laser electronics.

2.4. Sample preparation

Matrix and analyte crystalline sample films were prepared as reported previously [4]. Peptides gramicidin S (G-5001, Sigma, St. Louis, MO, USA) and bradykinin (B-3259, Sigma) and proteins bovine insulin (I-5500, Sigma) and cytochrome C (C-2506, Sigma) were used as analytes. MALDI matrices were 4-nitroaniline (72680, Fluka, Buchs, Switzerland), 2,5-dihydroxybenzoic acid (G5254, Sigma), sinapinic acid (D7927, Sigma), and α-cyano-4-hydroxycinnamic acid (C2020, Sigma). All reagents were used as purchased without further purification. DHB and NA were dissolved in methanol at a concentration of 50 mg/mL; SA and CCA were dissolved in a 50/50 (v/v) methanol:acetonitrile mixture at a concentration of 50 mg/mL. Analyte solutions were prepared by dissolving peptide and protein samples in 95/5 (v/v) methanol:1% trifluoroacetic acid (TFA, 04902-100, Fisher Scientific International, Pittsburgh, PA, USA) to a concentration of 500 μM. A 10 μL aliquot of analyte solution was mixed with a 10 μL aliquot of the matrix solutions. The total volume of the mixture was deposited on the sample target and dried with a heat gun for 15 s at a distance of 10 cm from the sample target surface. The dried sample was homogeneous and covered the entire area of the 8 mm diameter sample target and was approximately 80 μm thick.

3. Results and discussion

Two-laser LDI and MALDI was tested with four MALDI matrices and the analytes gramicidin S, bradykinin, bovine insulin, and cytochrome C. Two-laser matrix and analyte ion signal was obtained with DHB and SA; no two-laser matrix or analyte ion signal was found for samples prepared with CCA matrix. With the NA matrix, a high intensity matrix ion signal was observed for a matrix fragment, but no two-laser analyte ion signal was observed. In general, analyte signal was lower and more difficult to reproduce for peptides compared to proteins.

Mass spectra for bovine insulin (M_r = 5733.5 Da) in DHB matrix are shown in Fig. 1. The UV laser fluence is 55% of the one-laser threshold, and the IR laser fluence is at the one-laser threshold. At a delay of −100 ns (Fig. 1a; UV fired before IR), matrix and analyte ion signal result from the IR laser only. At delay times between 0 and several hundred nanoseconds, matrix and analyte ion signal are significantly larger. A typical two-laser mass spectrum obtained at a delay of 200 ns is shown in Fig. 1b; this mass spectrum is indicative of those obtained between 0 and 400 ns. One-laser mass spectra similar to the two-laser mass spectrum in Fig. 1b can be obtained if either the IR or the UV laser fluence alone is increased above the one-laser threshold.

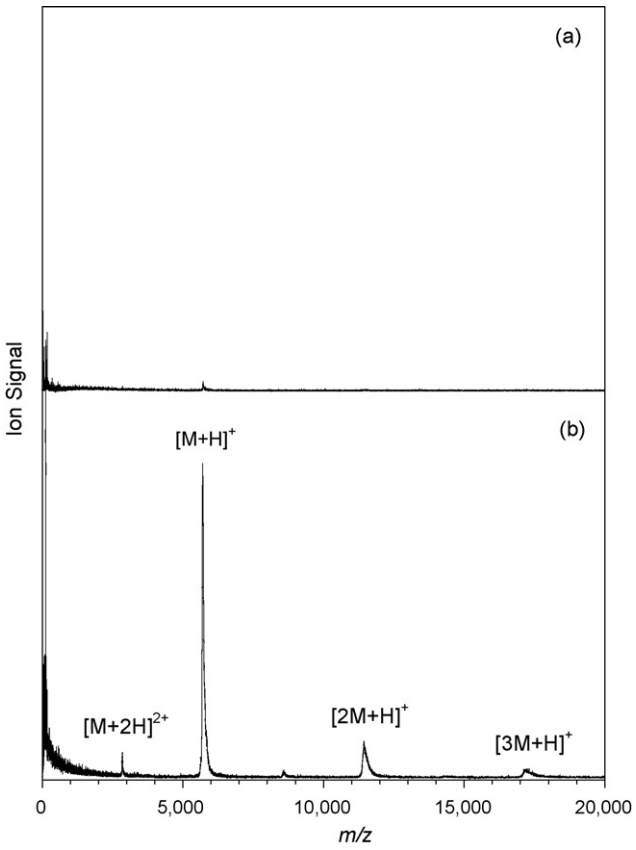

Fig. 1. Mass spectra of bovine insulin in DHB matrix obtained with 2.94 μm IR and 337 nm UV lasers at (a) $\Delta t = -100$ ns and (b) $\Delta t = 200$ ns. The UV laser fluence is 55% of one-laser threshold and the IR laser fluence is 100% of threshold. Negative delay times indicate the UV laser is firing before the IR laser.

Fig. 2 shows the mass spectra of bovine insulin in SA matrix. The UV laser is at threshold, and the IR laser fluence is at the threshold to produce matrix ions. No analyte ions were produced at any IR laser fluence using SA matrix and one-laser ionization. At a delay of −100 ns, matrix ion signal in Fig. 2a is from the UV and IR lasers, and analyte ion signal is from the UV laser only. Fig. 2b shows a mass spectrum obtained at 200 ns that is indicative of the two-laser mass spectra obtained between 0 and 400 ns. The SA two-laser mass spectrum is similar to the DHB two-laser mass spectrum, with the exception that the analyte cluster signal is significantly lower and the resolving power greater in the former case. A UV one-laser mass spectrum similar to Fig. 2b can be obtained if the UV laser fluence is increased, but, as indicated above, no IR one-laser mass spectrum could be obtained. The mass resolving power for SA in the one-laser case is also a factor of two greater than for one-laser UV MALDI with DHB, suggesting that the resolution difference is not related to a two-laser process.

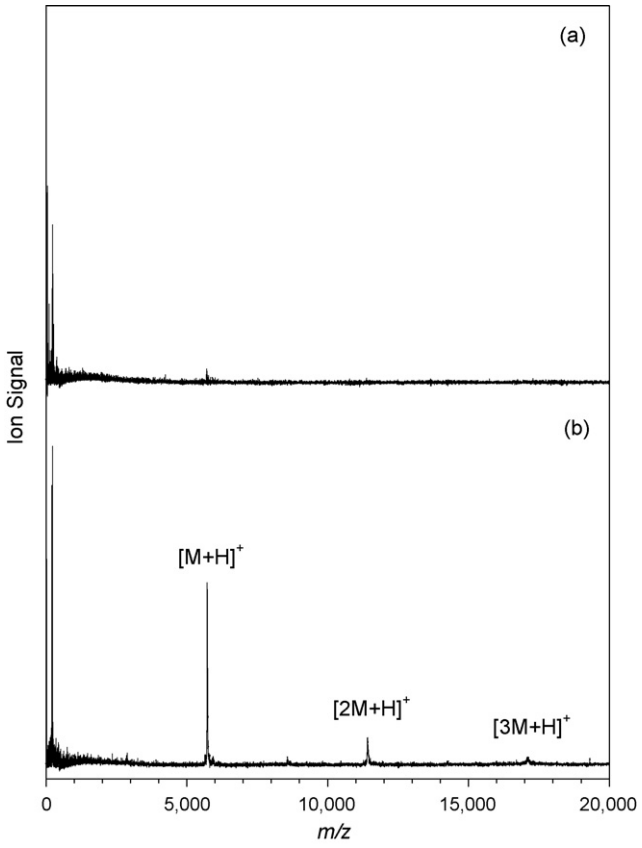

Fig. 2. Mass spectra of bovine insulin in SA matrix obtained with 2.94 μm IR and 337 nm UV lasers at (a) $\Delta t = -100$ ns and (b) $\Delta t = 200$ ns. The UV and IR lasers are at 100% of the one-laser threshold fluence.

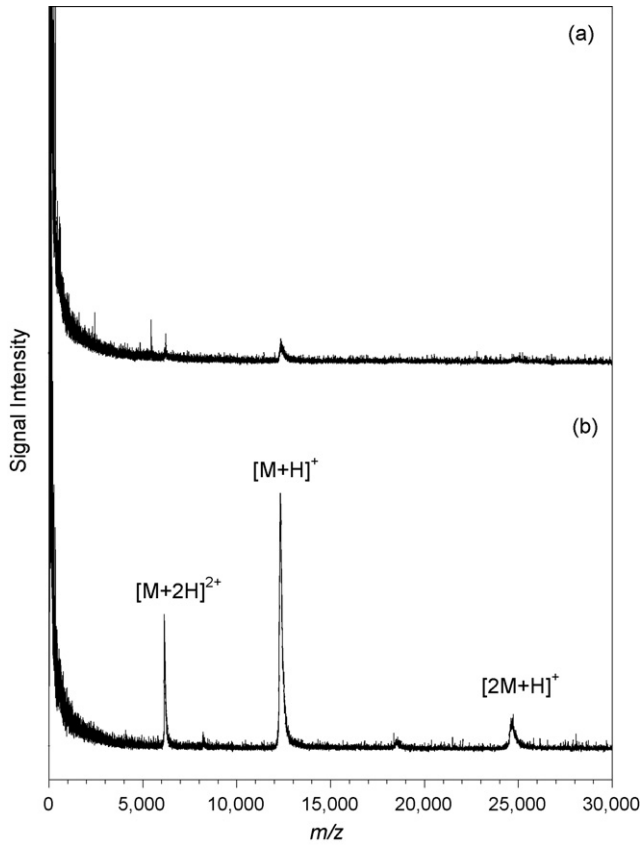

Fig. 4. Mass spectra of cytochrome C in DHB matrix obtained with IR and UV lasers at (a) $\Delta t = 0$ ns and (b) $\Delta t = 200$ ns. The UV and IR lasers are at 100% of one-laser threshold fluence.

In some cases, the two-laser signal was steady over time and plots of integrated signal intensity as a function of time could be obtained. In Fig. 3, the peak area for the $[M+H]^+$ ion of bovine insulin in SA matrix is plotted as a function of delay. The non-zero baseline is due to detector noise and does not indicate analyte ion signal at negative delay times. Two-laser analyte ion signal is observed at zero delay and continues at approximately the same intensity to 400 ns and then drops to baseline after 700 ns. The higher baseline after 700 ns does not appear to be associated with analyte ion signal and may be caused by thermionic emission or gas phase UV ionization of neutrals ejected from the target by the IR laser. In contrast to SA, it was not possible to obtain reproducible delay plots for bovine insulin in DHB matrix. The large variation in the DHB ion signal may be due to the higher IR laser fluence that was required to obtain two-laser signal.

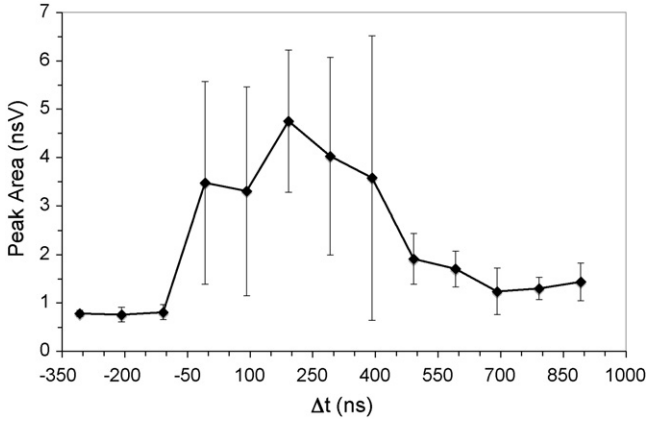

Fig. 3. Integrated singly protonated ion signal as a function of delay time for bovine insulin in SA matrix from −300 to 900 ns in 100 ns increments. Error bars represent one standard deviation.

Two-laser ion signal was observed for cytochrome C ($M_r = 12{,}384$ Da) in DHB matrix as shown in Fig. 4. Results are similar to bovine insulin in DHB matrix (Fig. 1). Fig. 4a was obtained by adjusting the delay such that the two-laser signal was at a minimum yet the IR and UV laser fluence was sufficient to achieve two-laser MALDI. At these fluences it was not possible to entirely eliminate the one-laser signal. The mass spectrum in Fig. 4b was obtained at 200 ns and is indicative of the two-laser signal observed at positive delay times. One-laser IR and UV MALDI spectra (similar to the mass spectrum in Fig. 4b) can be obtained at higher laser fluences.

The NA matrix was unique in that the one-laser and two-laser matrix mass spectra were different. Fig. 5 shows mass spectra for 4-nitroaniline ($M_r = 138.1$ Da). The UV laser fluence is 20% of threshold. No one-laser IR LDI signal was detected for NA at any IR laser fluence; therefore, the IR laser energy was attenuated to the minimum energy necessary for two-laser LDI at 50 ns. At a delay of −10 ns, no matrix or analyte ion signal is observed

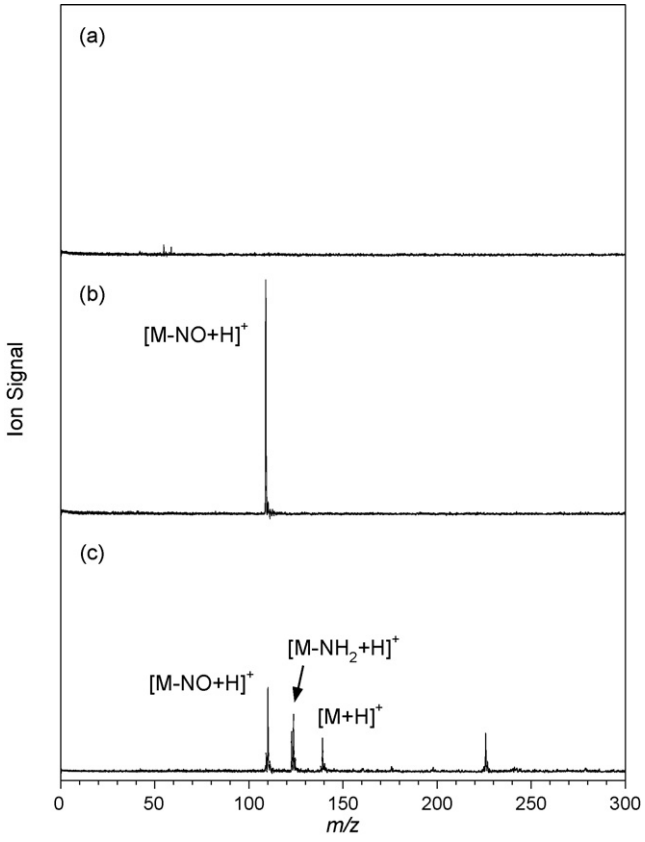

Fig. 5. Mass spectra of 4-nitroaniline matrix obtained with (a) IR and UV lasers at $\Delta t = -10$ ns, (b) IR and UV lasers at $\Delta t = 50$ ns and (c) a UV laser alone. The UV laser fluence is 20% of threshold and the IR laser fluence is the minimum required to produce two-laser matrix ions.

(Fig. 5a). At a delay of 50 ns, a mass spectrum is observed with a single peak corresponding to the protonated fragment of 4-nitroaniline after the loss of NO (Fig. 5b). No two-laser signal was observed for analyte at any fluence. When the UV fluence is increased to threshold, a different mass spectrum is obtained. The one-laser UV LDI mass spectrum for NA is shown in Fig. 5c, which was obtained at the one-laser threshold fluence. The most intense peak is the protonated NO loss fragment, but there are peaks corresponding to the NH_2 loss fragment, the protonated matrix and a fragment dimer at m/z 217. The $[M - NO + H]^+$ signal was intense and reproducible and was used to obtain the delay plot shown in Fig. 6. The signal rises rapidly beginning at zero delay to a maximum near 100 ns and then returns to baseline after approximately 500 ns.

In a previous study from this laboratory, it was postulated that the function of the IR laser in two-laser ionization is to heat the sample and thereby increase the ionization efficiency of UV desorption ionization. It is unlikely that excited electronic state processes are important in two-laser IR/UV LDI as they are in two-laser and two-pulse UV/UV LDI [1–3]. It is possible that the IR laser heats the sample to its melting point. The melting points for the solid matrices used in this study range from 421 to 537 K [8]. Temperatures of 600–800 K are normally sufficient to produce alkali metal ions by thermionic emission [9]. The presence of sodium positive ions in the IR LDI mass spectra at

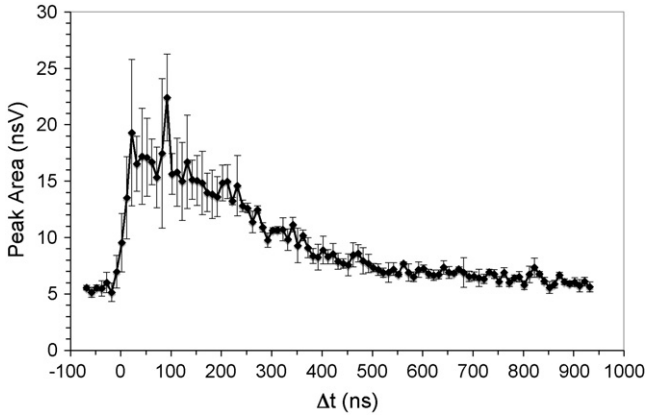

Fig. 6. Integrated ion signal for the NO loss fragment of 4-nitroaniline plotted as a function of delay time from −70 to 950 ns in 10 ns increments. Error bars represent one standard deviation.

two-laser ionization fluences suggests that the temperature following IR irradiation is sufficient for matrix melting. The lack of observed two-laser ionization with the CCA matrix may be due to the relatively low absorption of that matrix at 2.94 μm. A thin film of CCA has an IR absorption peak at 3.02 μm and a relatively low absorption at 2.94 μm [10]. In contrast, SA, NA and DHB have a comparatively larger absorption at that wavelength. Although the lack of absorption coefficients for crystalline solids data makes it difficult to make quantitative, rough estimates can be made. The energy deposition per molecule can be estimated using the Beer–Lambert Law and assuming negligible light scattering from the surface [11]

$$\frac{E}{N} = 2.3(1 - R)\frac{\varepsilon}{N_A}H$$

where R is the surface reflectance, ε the absorption coefficient, c the molar concentration of matrix, N_A the Avogadro's number, and H is the fluence. Using an estimated absorption coefficient [11] of 20 and 40 $M^{-1}\,cm^{-1}$ and a fluence of 2100 J/m^2, a volumetric energy of approximately 10 kJ/mol (about 0.1 eV per molecule) is obtained. The heat of fusion for benzoic acid is 18 kJ/mol [12] and this should be similar to that of the matrix molecules. This calculation suggests that available energy is close to the matrix melting point and that small changes in absorption coefficient may affect the two-laser processes.

The time behavior of the two-laser LDI is consistent with the one-dimensional heating model presented in the previous two-laser MALDI MS study that used a CO_2 laser as the IR source [4]. That model predicts that the maximum target temperature will occur at the end of the IR laser pulse. In the CO_2 laser study, the full pulse is 900 ns, which coincides with the maximum in the two-laser signal for both matrix and analyte. In the current study, the IR laser pulse width is 5 ns and ion signal was observed to be coincident with the end of the IR pulse within the 40 ns jitter in the delay measurement.

The drop in two-laser ion signal is interpreted as reflecting the drop in the surface temperature after the IR laser heating. In the previous study, the time for the return to baseline signal was between 100 and 300 μs; in the current study, the return to zero

occurs within 1 μs. This difference is most likely due to the slow heating of the stainless steel substrate by the 10.6 μm laser as compared to the rapid heating of the matrix by the 2.9 μm laser. The bulk metal will cool more slowly than the thin matrix film. An alternate explanation for the rapid return to baseline is that the UV laser is interacting with the expanding plume of material desorbed by the IR laser. Given a 500 m/s plume velocity, the UV laser would be expected to interact with ablated material for 100 ns or more after the IR ablation [1]. As the plume moves out of the UV laser field of view, this plume irradiation will no longer be possible. However, the flight times of the matrix and analyte ions formed by two-laser MALDI are constant to better than 0.2%, suggesting that they are formed at the surface rather than in the gas phase above the target. The anomalous two-laser mass spectrum for NA might be better explained by its high vapor pressure compared to the other matrices [13] which could lead to a dense plume after IR laser heating. A high collision number in this dense plume could explain the high degree of fragmentation in the two-laser mass spectrum.

4. Conclusion

Two-laser MALDI MS studies were performed using an OPO laser operating at 2.94 μm for the IR source and a 337 nm nitrogen laser for the UV source. Two-laser matrix and analyte signal was found for DHB and SA matrices but not for CCA matrix. Two-laser mass LDI signal was observed for NA matrix, but the mass spectrum is not the same as the one-laser UV LDI mass spectrum. The two-laser signal occurs when the IR and UV lasers are fired simultaneously (with 40 ns jitter) and can be obtained for delay times between the IR and UV laser of up to 500 ns. The results are interpreted as rapid heating and possibly melting of the matrix followed by efficient UV MALDI from the heated sample.

Acknowledgements

This work was supported by the National Science Foundation CHE-0415360. The authors thank Dr. David Rousell for many helpful discussions.

References

[1] X. Tang, M. Sadeghi, Z. Olumee, A. Vertes, Rapid Commun. Mass Spectrom. 11 (1997) 484.
[2] R. Knochenmuss, A. Vertes, J. Phys. Chem. B 104 (2000) 5406.
[3] E. Moskovets, A. Vertes, J. Phys. Chem. B 106 (2002) 3301.
[4] M.W. Little, J.K. Kim, K.K. Murray, J. Mass Spectrom. 38 (2003) 772.
[5] M. Schürenberg, K. Dreisewerd, S. Kamanabrou, F. Hillenkamp, Int. J. Mass Spectrom. Ion Process. 172 (1998) 89.
[6] W.E. Wallace, M.A. Arnould, R. Knochenmuss, Int. J. Mass Spectrom. Ion Process. 242 (2005) 13.
[7] K.L. Caldwell, K.K. Murray, Appl. Surf. Sci. 127–129 (1998) 242.
[8] D.R. Lide (Ed.), CRC Handbook of Chemistry and Physics, 81st ed., CRC Press, Boca Raton, FL, 2000.
[9] G.J.Q. Van der Peyl, J. Haverkamp, P.G. Kistemaker, Int. J. Mass Spectrom. Ion Phys. 42 (1982) 125.
[10] V.L. Talrose, M.D. Person, R.M. Whittal, F.C. Walls, A.L. Burlingame, M.A. Baldwin, Rapid Commun. Mass Spectrom. 13 (1999) 2191.
[11] D. Feldhaus, C. Menzel, S. Berkenkamp, F. Hillenkamp, K. Dreisewerd, J. Mass Spectrom. 35 (2000) 1320.
[12] Data from NIST, Standard Reference Database 69, June 2005 Release: NIST Chemistry, WebBook.
[13] Vapor pressures were obtained from CAS Scifinder and were calculated using Advanced Chemistry Development (ACD/Labs) Software V8.14 for Solaris.